PHYSICAL REVIEW A **91**, 060502(R) (2015)

Dual Fano and Lorentzian line profile properties of autoionizing states

B. Tu,[1] J. Xiao,[1] K. Yao,[1] Y. Shen,[1] Y. Yang,[1] D. Lu,[1] W. X. Li,[1] M. L. Qiu,[1] X. Wang,[1] C. Y. Chen,[1] Y. Fu,[1] B. Wei,[1] C. Zheng,[1] L. Y. Huang,[1] B. H. Zhang,[2] Y. J. Tang,[2] R. Hutton,[1] and Y. Zou[1,*]

[1]*Shanghai EBIT Laboratory, Institute of Modern Physics, Fudan University and the Key Laboratory of Applied Ion Beam Physics, Chinese Ministry of Education, Shanghai 200433, China*

[2]*Research Center of Laser Fusion, China Academy of Engineering Physics, P.O. Box 919-986, Mianyang 621900, China*

(Received 3 December 2014; published 22 June 2015)

Photon absorption spectroscopy is a powerful tool for uncovering the structure of atoms, molecules, and solids. Symmetric Lorentzian and asymmetric Fano line shapes are fundamental spectroscopic signatures related to the structural and dynamical properties. Recently, Ott *et al.* [Science **340**, 716 (2013)] successfully transferred Fano profile into Lorentzian line shape using an intense infrared laser, after excitation of autoionizing states in helium by attosecond XUV pulse. This is a very important step forward in quantum phase control. However, here we show experimentally that an autoionizing state can have both Fano and Lorentzian behavior naturally, depending on the process involved. This study utilized the inverse process of photon absorption ionization, i.e., electron ion recombination with photon emission, making sure the resonant autoionizing state is not modified or decorated by the laser fields. Our result implies that excitation of the state through different paths—for example, one photon versus multiphoton excitation, or even one step versus multistep excitation—can lead to different Fano profiles for the same resonant state. We also report an experimental determination of the energy shifts in the recombination photon-intensity peaks due to the interference between the resonant and nonresonant processes.

DOI: 10.1103/PhysRevA.91.060502 PACS number(s): 32.70.Jz, 32.80.Fb, 32.80.Aa, 32.80.Zb

Asymmetric Fano absorption line shapes emerge when discrete excited states are coupled to the continuum [1,2]. Such asymmetric resonances are ubiquitous in essentially all fields, through nuclear [3], atomic [4–7], molecular [8] to solid-state physics [9–12]. Coupling (or configuration interaction) of discrete and continuum states is a problem of electron-electron interaction, or electron-electromagnetic field interaction. The advanced laser technology nowadays allows scientists to simulate, modify, or even cancel some of the interactions, as was done in the work of Ott *et al.* [13], and finally could lead to many important applications [14–17], especially in the field of quantum control.

Electron ion recombinations, both resonant and nonresonant, are inverse processes of atomic photon absorption ionization. Dielectronic recombination (DR), as the main process of resonant recombination, is considered as a two-step process. In the first step a free electron is captured by an ion, and a bound electron in the ion is promoted, forming an intermediate doubly or even multiply excited state sitting above the ionization threshold (this kind of state is also called an autoionizing state). In the second step, photons are emitted to reduce the energy of the recombined ion to below its ionization limit, so as to stabilize this recombination. The first step endows DR the resonant character and determines the resonant energy, i.e., only when the energy released from the capture of the free electron matches the excitation energy of the promoted electron can the DR process happen. The second step can lead the recombined ion to different final states according to the transition branching ratio. While in the nonresonant recombination, also named as radiative recombination (RR), a free electron is captured by an ion and the excess energy is released directly by emitting a photon [see Fig. 1(a)]. DR and RR are also important in high temperature plasmas, such as celestial or fusion plasmas. They affect the charge state balance, degrade the plasma temperature, and produce lots of satellite lines, some of which are very useful in plasma diagnostics. Much work has been done to study these processes (see [18–22], and references therein), but only very few have observed interference between the DR and RR [23–26], due to the fact that most studies were for the cases where RR was much weaker than DR, and the interference was negligible.

In order to study the variation of the Fano profile (consequently, the Fano parameter) of a given autoionizing state, we selected the DR resonances which go through an intermediate state with decay channels to both the final states with no excited electrons [Fig. 1(b)] and the final states with more than one electron in excited orbit [Fig. 1(c)]. In the former case, both dielectronic and radiative recombination will occur; interference and hence the asymmetric line profile should be expected. In the latter case, only dielectronic recombination (so no interference) will take place; because the radiative recombination process does not change the orbital occupation of the recombining ion, it cannot end up in a final state with more than one electron in the excited state when RR happens between an electron and an ion in the ground state. In detail, we studied the DR processes of (1) C-like tungsten (W) ions, through the intermediate state of $[1s2s^22p_{1/2}^2(2p_{3/2}^2)_2]_{5/2}$ to two different sorts of final states, $[1s^22s^22p_{1/2}^22p_{3/2}]$ and $[1s^22s^22p_{1/2}(2p_{3/2}^2)_2]_{(3/2,5/2)}$; (2) N-like W ions through the intermediate state of $[1s2s^22p_{1/2}^2(2p_{3/2}^3)_{3/2}]_2$, to two different sorts of final states $[1s^22s^22p_{1/2}^2(2p_{3/2}^2)_{(0,2)}]_{(0,2)}$ and $[1s^22s^22p_{1/2}(2p_{3/2}^3)_{3/2}]_{(1,2)}$; and (3) O-like W ions through $[1s2s^22p_{1/2}^2(2p_{3/2}^4)_0]_{1/2}$ to $[1s^22s^22p_{1/2}^2(2p_{3/2}^3)_{3/2}]_{3/2}$

*zouym@fudan.edu.cn

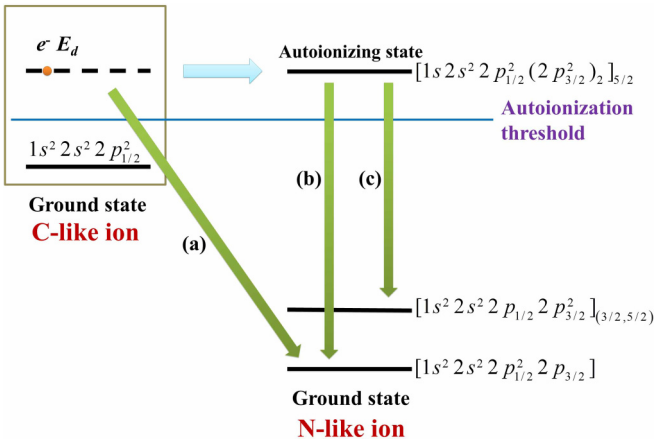

FIG. 1. (Color online) Energy level diagram of electron ion recombination for C-like ions. (a) shows the radiative recombination of an electron with a C-like ion in the ground state, to form the N-like state $[1s^22s^22p_{1/2}^22p_{3/2}]$. (b) and (c) show the dielectronic recombination of an electron with a C-like ion in the ground state, to form the N-like states of $[1s^22s^22p_{1/2}^22p_{3/2}]$ and $[1s^22s^22p_{1/2}(2p_{3/2}^2)_2]_{(3/2,5/2)}$ respectively, through the same autoionizing state of $[1s2s^22p_{1/2}^2(2p_{3/2}^2)_2]_{5/2}$.

and $[1s^22s^22p_{1/2}(2p_{3/2}^4)_0]_{1/2}$. In all these cases, the $2p_{1/2}$ orbit is lower than $2p_{3/2}$ in energy.

The experiment was done at the Shanghai electron beam ion trap [27] (Shanghai EBIT). The setup and method in this work were similar to those described in our previous paper [20,28,29] for DR studies of Xe ions. During the experiment, $W(CO)_6$ was continuously injected into the EBIT, and a plasma with ions from W, C, and O was produced in the trap region. The electron energy was adjusted as shown in Fig. 2, to produce the right charge states of W ions, and to scan through the DR resonances of interest. The event mode data acquisition system was triggered by an x-ray photon (from the recombination event), then the photon energy and the corresponding electron energy were simultaneously recorded as shown in Fig. 3. In Fig. 3, the resonant peaks are from KL_3L_3 DR events, in which a free electron was captured to L_3 at the same time a K-shell electron in the ion was promoted to L_3 (L_3 means the $2p_{3/2}$ orbit), of Be-, B-, C-, N-, and O-like W ions. The events on the clear diagonal band correspond to the RR processes to the final states of principal quantum number $n = 2$, and the total angular momentum $J = 3/2$ of these ions.

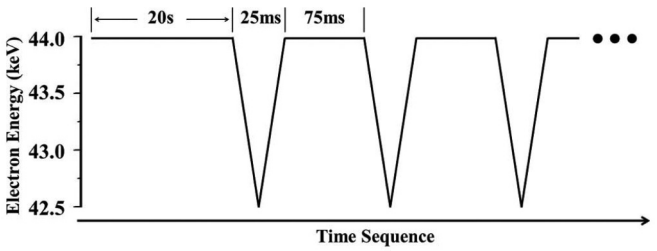

FIG. 2. Time sequence for electron beam energy adjustment in the present experiment.

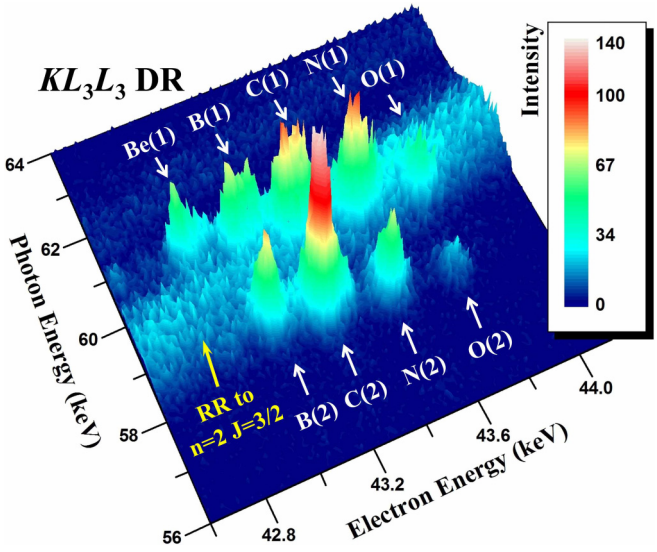

FIG. 3. (Color online) Three-dimensional spectrum for the electron ion recombination of W ions. The peaks are from KL_3L_3 DR events of Be-, B-, C-, N-, and O-like W ions. The events on the diagonal band correspond to the RR processes to the final states of principal quantum number $n = 2$, and the total angular momentum of $J = 3/2$ of these ions. The events in C(1) are from the DR processes through the autoionizing states of $[1s2s^22p_{1/2}^2(2p_{3/2}^2)_2]_{5/2}$, $[1s2s^22p_{1/2}^2(2p_{3/2}^2)_2]_{3/2}$, and $[1s2s^22p_{1/2}^2(2p_{3/2}^2)_0]_{1/2}$, to the final ground state of $[1s^22s^22p_{1/2}^22p_{3/2}]_{3/2}$. Those in C(2) are through the same intermediate states, but to the final states with two electrons on the excited orbit $2p_{3/2}$. The events in N(1) and N(2) are from the DR processes of N-like W ions through the same intermediate states $[1s2s^22p_{1/2}^2(2p_{3/2}^3)_{3/2}]_2$ and $[1s2s^22p_{1/2}^2(2p_{3/2}^3)_{3/2}]_1$, to the final ground state and the final state with three electrons on the excited orbit of $2p_{3/2}$. The events of O(1) and O(2) are from the DR of O-like W ions, with O(1) for the processes through $[1s2s^22p_{1/2}^2(2p_{3/2}^4)_0]_{1/2}$ to the final ground state $[1s^22s^22p_{1/2}^2(2p_{3/2}^3)_{3/2}]_{3/2}$, and O(2) through the same intermediate state to the final state with four electrons on the excited orbit $2p_{3/2}$.

The events marked as C(1) in Fig. 3 are from the DR processes of C-like W ions through autoionizing states of $[1s2s^22p_{1/2}^2(2p_{3/2}^2)_2]_{5/2}$, $[1s2s^22p_{1/2}^2(2p_{3/2}^2)_2]_{3/2}$, and $[1s2s^22p_{1/2}^2(2p_{3/2}^2)_0]_{1/2}$, to the final state of $[1s^22s^22p_{1/2}^22p_{3/2}]_{3/2}$. Those designated as C(2) are through the same intermediate states, but to the final states with two electrons in the excited orbit of $2p_{3/2}$, $[1s^22s^22p_{1/2}(2p_{3/2}^2)_2]_{3/2}$, $[1s^22s^22p_{1/2}(2p_{3/2}^2)_2]_{5/2}$, and $[1s^22s^22p_{1/2}(2p_{3/2}^2)_0]_{1/2}$. The last final state is only from the $[1s2s^22p_{1/2}^2(2p_{3/2}^2)_0]_{1/2}$. The events in C(1) and C(2) were then picked out along the $n = 2$, $J = 3/2$ RR band and projected onto the electron energy axis, as was done in [24], to produce excitation functions of electron ion recombination for the two cases, shown in Figs. 4(a) and 4(b), respectively. Figure 4(a) shows asymmetric line profiles; Fig. 4(b) does not. It is obvious as C(1) sits on the RR band (so interference occurs), but C(2) not. We made a least-squares fitting for the excitation function in Fig. 4(b), employing a Lorentzian

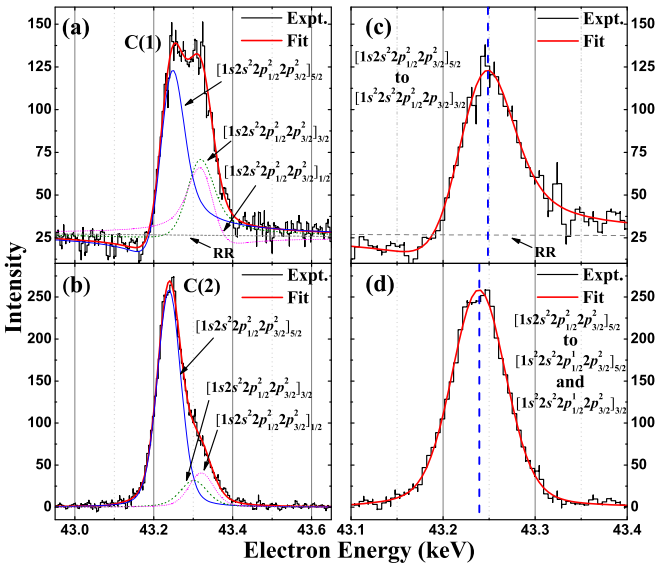

FIG. 4. (Color online) The excitation functions of the KL_3L_3 DR spectra of C-like W ions through the interference channel (a) and noninterference channel (b). The intermediate autoionizing states are labeled for each resonance in (a) and (b). (a) shows an asymmetric line profile, which indicates the occurrence of the interference between the DR and RR. (b) shows a symmetric line shape, which implies that no interference is involved. (c) and (d) show the enlarged peak of the DR resonance through the autoionizing state of $[1s2s^22p^2_{1/2}(2p^2_{3/2})_2]_{5/2}$ for the interference and noninterference channel, respectively, after subtracting the contribution from the two unresolvable resonances, $[1s2s^22p^2_{1/2}(2p^2_{3/2})_2]_{3/2}$ and $[1s2s^22p^2_{1/2}(2p^2_{3/2})_0]_{1/2}$, according to the least-squares fitting result. The energy shift of the peak in the x-ray intensity caused by the interference can be seen clearly in (c), comparing the peak position in (d).

Gaussian convoluted profile as expressed in the following, to account for the small electron energy spread in the EBIT.

$$C(E) = \int_{-\infty}^{+\infty} L(E')G(E'-E)dE' = A\frac{2\ln 2\Gamma_d}{w^2\pi\sqrt{\pi}}\int_{-\infty}^{+\infty}\frac{e^{-t^2}}{(t-x)^2+y^2}dt, \quad (1)$$

$$t = \frac{2\sqrt{\ln 2}(E'-E)}{w}; \quad x = \frac{2\sqrt{\ln 2}(E_d-E)}{w};$$

$$y = \frac{\sqrt{\ln 2}\Gamma_d}{w}, \quad (2)$$

where $L(E')$ and $G(E'-E)$ are Lorentzian and Gaussian distribution functions, respectively. A denotes the peak area, Γ_d the total width of the resonant state, w the full width at half maximum of electron energy distribution described by the Gaussian function, and E_d denotes the resonant energy. The obtained resonant energies and the width of the Gaussian distribution (which is 61 eV) were then used as fixed parameters, to fit the data in Fig. 4(a), utilizing a Fano Gaussian convoluted profile [30] (see the following), as in this case interference is involved.

$$C(E) = \int_{-\infty}^{+\infty} F(E')G(E'-E)dE' = \frac{2A}{q^2\Gamma_d\pi\sqrt{\pi}} \times \int_{-\infty}^{+\infty}\left[\frac{(qy+t-x)^2+(B_a-1)^2y^2}{(t-x)^2+y^2}-1\right]e^{-t^2}dt. \quad (3)$$

Here $F(E')$ is the distribution function for a Fano profile, q is the Fano parameter, and $B_a = \Gamma_a/\Gamma_d$ is the branch ratio for autoionization of the resonant state, obtained by relativistic configuration interaction calculation. The resonances for $[1s2s^22p^2_{1/2}(2p^2_{3/2})_2]_{3/2}$ and $[1s2s^22p^2_{1/2}(2p^2_{3/2})_0]_{1/2}$ are too close to resolve, and they are not subjects for this study. The resonance for $[1s2s^22p^2_{1/2}(2p^2_{3/2})_2]_{5/2}$ is just far enough from the unresolvable ones, to obtain reliable results. Our data analysis led to a Fano parameter of 4.4 (0.4) for the interference channel through this autoionizing state. This agrees very well with our theoretical result of 4.3, based on the relativistic configuration interaction method (RCI), using the flexible atomic code [31]. Comparing the peak positions of the interference and noninterference channels in Figs. 4(a) and 4(b) [clearer seen in Figs. 4(c) and 4(d)], the electron energy shift of the peak in the x-ray intensity, caused by the interference, was obtained in electron ion recombination, with a value of 9.8 (0.8) eV. The results are listed in Table I.

The events in N(1) in Fig. 3 are from the DR processes of N-like W ions through autoionizing states of $[1s2s^22p^2_{1/2}(2p^3_{3/2})_{3/2}]_2$ and $[1s2s^22p^2_{1/2}(2p^3_{3/2})_{3/2}]_1$ to the final state of $[1s^22s^22p^2_{1/2}(2p^2_{3/2})_2]_2$ and $[1s^22s^22p^2_{1/2}(2p^2_{3/2})_0]_0$. The final state with total angular momentum $J=0$ is only from the intermediate state of $[1s2s^22p^2_{1/2}(2p^3_{3/2})_{3/2}]_1$. Those marked as N(2) are from the same autoionizing state but to different final states of $[1s^22s^22p_{1/2}(2p^3_{3/2})_{3/2}]_1$ and $[1s^22s^22p_{1/2}(2p^3_{3/2})_{3/2}]_2$. The events of O(1) and O(2) are from the DR of O-like W ions, with O(1) for the processes through $[1s2s^22p^2_{1/2}(2p^4_{3/2})_0]_{1/2}$ to $[1s^22s^22p^2_{1/2}(2p^3_{3/2})_{3/2}]_{3/2}$, and O(2) through the same intermediate state to the final state of $[1s^22s^22p_{1/2}(2p^4_{3/2})_0]_{1/2}$. Using the same procedure described above for C-like W, the Fano parameters and energy shifts were obtained for the resonances of N-like W through the autoionizing state of $[1s2s^22p^2_{1/2}(2p^3_{3/2})_{3/2}]_2$ to $[1s^22s^22p^2_{1/2}(2p^2_{3/2})_2]_2$, and for the O-like W through $[1s2s^22p^2_{1/2}(2p^4_{3/2})_0]_{1/2}$ to $[1s^22s^22p^2_{1/2}(2p^3_{3/2})_{3/2}]_{3/2}$. They are also listed in Table I. The measured Fano parameters agree very well with our RCI calculations. The resonance for N-like W through $[1s2s^22p^2_{1/2}(2p^3_{3/2})_{3/2}]_1$ has two transition channels in the case with interference, and they are not separable in this study, so it is not possible to reach a reliable result for their Fano parameters and phase shifts in this case.

Although the two-step model has been quite successful in calculating DR processes, it is no longer able to provide good description when interference is involved, and a unified theory [32–39] takes its place in dealing with the interfering radiative and dielectronic recombination. The theoretical predictions show two effects concerning the interference: asymmetric line profile and energy shift for the maximum cross section.

TABLE I. The results of measured and calculated Fano parameters, together with the measured energy shifts of the peak in the x-ray intensities for the resonances of C-like, N-like, and O-like W ions. The experimental uncertainties are listed in parentheses.

Charge state	Middle state	Final state	q_{meas}	E_{shift} (eV)	q_{theor}
C-like	$[1s2s^22p_{1/2}^2(2p_{3/2}^2)_2]_{5/2}$	$[1s^22s^22p_{1/2}^2 2p_{3/2}]_{3/2}$	4.4(0.4)	9.8(0.8)	4.3
N-like	$[1s2s^22p_{1/2}^2(2p_{3/2}^3)_{3/2}]_2$	$[1s^22s^22p_{1/2}^2(2p_{3/2}^2)_2]_2$	13.4(2.1)	3.5(0.6)	13.7
O-like	$[1s2s^22p_{1/2}^2(2p_{3/2}^4)_0]_{1/2}$	$[1s^22s^22p_{1/2}^2(2p_{3/2}^3)_{3/2}]_{3/2}$	11.8(1.6)	4.3(0.8)	10.5

Previous experiments [23–26] observed only the asymmetric line profiles, while in this work we have successfully observed and determined both the asymmetric line profile and the energy shift.

In this work, the autoionizing state involved in both channels with and without interference for each charge state are the same state, so should be described by the same wave function and hence the same mixing of discrete and continuum configurations. The very different Fano parameters—4.4 and infinite for C-like, 13.4 versus infinite for N-like, and 11.8 versus infinite for the O-like case—indicates that an autoionizing state can have both Fano and Lorentzian behavior naturally, depending on the process involved.

Although coupling of a discrete state with the continuum is necessary for a Fano profile (without external disturbance), it does not mean that stronger coupling would lead to stronger Fano asymmetry. The Fano parameter is proportional to the relative strength of the DR over RR in electron ion recombination, or proportional to the relative strength of the indirect (resonant) ionization over the direct ionization in photon absorption. It is a measure of the degree of interference. The strongest asymmetric line profile, or the strongest interference, would occur when the strengths of the two interfering processes are about equal. With the absence of either partner, the interference will not occur, corresponding to the case of an infinite or a zero Fano parameter, and hence a vanishing Fano profile. But stronger coupling does mean stronger mixing of the continuum into the discrete, resulting from larger deviation from hydrogenic field for the electrons, which is usually seen in the cases where the two excited electrons are in close-lying quantum states. In the work by Ott *et al.* [13], they could successfully turn the Fano profile to Lorentzian for sp_{2n+} states with n above 3 for He, at the laser intensity of 2.0×10^{12} W/cm^2, but not for $2s2p$ and sp_{23+}. It could well be the reason that the laser intensity is not enough to compensate the effect of stronger coupling of the continuum to the discrete for the $2s2p$ and sp_{23+} cases. We could also expect that for sp_{2n+} with very high n, the absorption line shape would approach Lorentzian even without the laser compensation, because in this case the wave function could be very well described by hydrogenic function, i.e., almost no interaction with the continuum state. For the application to quantum control using the Fano/Lorentzian line profile of atomic states, we suggest to choose the resonant states with medium or relatively weak coupling between the discrete states and the continuum for easier implementation of laser field modification of the coupling, and to choose the process with similar strengths of both channels to get the highest dynamic range of the interference.

In conclusion, we have made experimental studies on the DR resonances with both interference and noninterference channels for several autoionizing states of C-like, N-like, and O-like W ions, by specially selecting the intermediate states with decay channels to both the final states with no excited electrons and the final states with more than one electron in excited orbits. By doing so, we have experimentally determined the energy shifts of the peak in the recombination photon intensity, at the same time as when the asymmetric line profiles were measured for the interference channels. Our result shows that an autoionizing state can have dual Fano and Lorentzian line profile properties naturally, depending on the process involved. Our result implies that excitation of the state through different paths—for example one photon versus multiphoton excitation, or even one step versus multistep excitation—can lead to different Fano profiles for the same resonant state.

The authors thank Dr. Sven Huldt and Dr. Tomas Brage for helpful comments. This work was supported by the National Magnetic Confinement Fusion Program with Grant No. 2015GB117000, Shanghai Leading Academic Discipline Project No. B107, and by Science and Technology Commission of Shanghai Municipality under Grant No. 13ZR1451500.

[1] U. Fano, Nuovo Cimento **12**, 154 (1935).
[2] U. Fano, Phys. Rev. **124**, 1866 (1961).
[3] J. M. Blatt and V. F. Weisskopf, *Theoretical Nuclear Physics* (Wiley, New York, 1952).
[4] U. Eichmann, T. F. Gallagher, and R. M. Konik, Phys. Rev. Lett. **90**, 233004 (2003).
[5] R. P. Madden and K. Codling, Phys. Rev. Lett. **10**, 516 (1963).
[6] U. Fano and J. W. Cooper, Rev. Mod. Phys. **40**, 441 (1968).
[7] J. M. Rost, K. Schulz, M. Domke, and G. Kaindl, J. Phys. B. **30**, 4663 (1997).
[8] S. H. Linn, W. B. Tzeng, J. M. Brom, and C. Y. Ng, J. Chem. Phys. **78**, 50 (1983).
[9] J. A. Fan, C. Wu, K. Bao, J. Bao, R. Bardhan, N. J. Halas, V. N. Manoharan, P. Nordlander, G. Shvets, and F. Capasso, Science **328**, 1135 (2010).

[10] A. R. Schmidt, M. H. Hamidian, P. Wahl, F. Meier, A. V. Balatsky, J. D. Garrett, T. J. Williams, G. M. Luke, and J. C. Davis, Nature (London) **465**, 570 (2010).
[11] M. Kroner, A. O. Govorov, S. Remi, B. Biedermann, S. Seidl, A. Badolato, P. M. Petroff, W. Zhang, R. Barbour, B. D. Gerardot, R. J. Warburton, and K. Karrai, Nature (London) **451**, 311 (2008).
[12] A. E. Miroshnichenko, S. Flach, and Y. S. Kivshar, Rev. Mod. Phys. **82**, 2257 (2010).
[13] C. Ott, A. Kaldun, P. Raith, K. Meyer, M. Laux, J. Evers, C. H. Keitel, C. H. Greene, and T. Pfeifer, Science **340**, 716 (2013).
[14] S. E. Harris, Phys. Today **50**(7), 36 (1997).
[15] A. H. Safavi-Naeini, T. P. M. Alegre, J. Chan, M. Eichenfield, M. Winger, Q. Lin, J. T. Hill, D. E. Chang, and O. Painter, Nature (London) **472**, 69 (2011).
[16] O. Kocharovskaya, Phys. Rep. **219**, 175 (1992).
[17] M. O. Scully, Phys. Rep. **219**, 191 (1992).
[18] S. Mahmood, S. Ali, I. Orban, S. Tashenov, E. Lindroth, and R. Schuch, Astrophys. J. **754**, 86 (2012).
[19] S. Schippers, D. Bernhardt, A. Müller, C. Krantz, M. Grieser, R. Repnow, A. Wolf, M. Lestinsky, M. Hahn, O. Novotný, and D. W. Savin, Phys. Rev. A **83**, 012711 (2011).
[20] K. Yao, Z. Geng, J. Xiao, Y. Yang, C. Chen, Y. Fu, D. Lu, R. Hutton, and Y. Zou, Phys. Rev. A **81**, 022714 (2010).
[21] A. J. González Martínez, J. R. Crespo López-Urrutia, J. Braun, G. Brenner, H. Bruhns, A. Lapierre, V. Mironov, R. Soria Orts, H. Tawara, M. Trinczek, J. Ullrich, A. N. Artemyev, Z. Harman, U. D. Jentschura, C. H. Keitel, J. H. Scofield, and I. I. Tupitsyn, Phys. Rev. A **73**, 052710 (2006).
[22] J. Clementson and P. Beiersdorfer, Astrophys. J **763**, 54 (2013).
[23] D. A. Knapp, P. Beiersdorfer, M. H. Chen, J. H. Scofield, and D. Schneider, Phys. Rev. Lett. **74**, 54 (1995).
[24] A. J. González Martínez, J. R. Crespo López-Urrutia, J. Braun, G. Brenner, H. Bruhns, A. Lapierre, V. Mironov, R. Soria Orts, H. Tawara, M. Trinczek, J. Ullrich, and J. H. Scofield, Phys. Rev. Lett. **94**, 203201 (2005).
[25] N. Nakamura, A. P. Kavanagh, H. Watanabe, H. A. Sakaue, Y. Li, D. Kato, F. J. Currell, X.-M. Tong, T. Watanabe, and S. Ohtani, Phys. Rev. A **80**, 014503 (2009).
[26] H. Tobiyama, H. Nohara, A. P. Kavanagh, N. Nakamura, H. Watanabe, H. A. Sakaue, Y. Li, D. Kato, F. J. Currell, C. Yamada, and S. Ohtani, J. Phys.: Conf. Ser. **58**, 239 (2007).
[27] D. Lu, Y. Yang, J. Xiao, Y. Shen, Y. Fu, B. Wei, K. Yao, R. Hutton, and Y. Zou, Rev. Sci. Instrum. **85**, 093301 (2014).
[28] W. D. Chen, W. Hu, Y. Q. Fu, J. Xiao, Y. Liu, F. C. Meng, T. M. Shen, C. Y. Chen, S. Wu, B. Wei, R. Hutton and Y. Zou, Phys. Plasmas **14**, 103302 (2007).
[29] W. D. Chen, J. Xiao, Y. Shen, Y. Q. Fu, F. C. Meng, C. Y. Chen, B. H. Zhang, Y. J. Tang, R. Hutton, and Y. Zou, Phys. Plasmas **15**, 083301 (2008).
[30] S. Schippers, S. Kieslich, A. Müller, G. Gwinner, M. Schnell, A. Wolf, A. Covington, M. E. Bannister, and L.-B. Zhao, Phys. Rev. A. **65**, 042723 (2002).
[31] M. F. Gu, Can. J. Phys. **86**, 675 (2008).
[32] S. L. Haan and V. L. Jacobs, Phys. Rev. A **40**, 80 (1989).
[33] K. J. LaGattuta, Phys. Rev. A **40**, 558 (1989).
[34] N. R. Badnell and M. S. Pindzola, Phys. Rev. A **45**, 2820 (1992).
[35] V. L. Jacobs, J. Cooper, and S. L. Haan, Phys. Rev. A **36**, 1093 (1987).
[36] F. Robicheaux, T. W. Gorczyca, M. S. Pindzola, and N. R. Badnell, Phys. Rev. A **52**, 1319 (1995).
[37] T. W. Gorczyca, M. S. Pindzola, F. Robicheaux, and N. R. Badnell, Phys. Rev. A **56**, 4742 (1997).
[38] D. M. Mitnik, M. S. Pindzola, and N. R. Badnell, Phys. Rev. A **59**, 3592 (1999).
[39] E. Behar, V. L. Jacobs, J. Oreg, A. Bar-Shalom, and S. L. Haan, Phys. Rev. A **69**, 022704 (2004).